Title

Matrix Metalloproteinase-9 Protects Islets from Amyloid-induced Toxicity*

Journal

Journal of Biological Chemistry, 290(51)

ISSN

0021-9258

Authors

Meier, Daniel T
Tu, Ling-Hsien
Zraika, Sakeneh
et al.

Publication Date

2015-12-01

DOI

10.1074/jbc.m115.676692

THE JOURNAL OF BIOLOGICAL CHEMISTRY VOL. 290, NO. 51, pp. 30475–30485, December 18, 2015
Published in the U.S.A.

Matrix Metalloproteinase-9 Protects Islets from Amyloid-induced Toxicity*

Received for publication, July 8, 2015, and in revised form, October 10, 2015 Published, JBC Papers in Press, October 19, 2015, DOI 10.1074/jbc.M115.676692

Daniel T. Meier[‡1,2], Ling-Hsien Tu[§¶1], Sakeneh Zraika[‡], Meghan F. Hogan[‡], Andrew T. Templin[‡3], Rebecca L. Hull[‡], Daniel P. Raleigh[¶‖], and Steven E. Kahn[‡4]

From the [‡]VA Puget Sound Health Care System and University of Washington, Seattle, Washington 98108, [§]Genomic Research Center, Academia Sinica, Taipei, Taiwan, [¶]Department of Chemistry, Stony Brook University, Stony Brook, New York 11794, and [‖]Department of Structural and Molecular Biology, University College London, London WC1E 6BT, United Kingdom

Background: MMP-9 cleaves hIAPP, the major constituent of islet amyloid deposits.
Results: MMP-9-cleaved hIAPP fragments are largely non-amyloidogenic and non-cytotoxic. MMP-9 overexpression in amyloid-prone islets reduces amyloid deposition and the associated toxicity.
Conclusion: MMP-9 protects islets from amyloid-induced toxicity.
Significance: MMP-9 activation specifically in islets might be a novel strategy to limit β-cell loss in type 2 diabetes.

Deposition of human islet amyloid polypeptide (hIAPP, also known as amylin) as islet amyloid is a characteristic feature of the pancreas in type 2 diabetes, contributing to increased β-cell apoptosis and reduced β-cell mass. Matrix metalloproteinase-9 (MMP-9) is active in islets and cleaves hIAPP. We investigated whether hIAPP fragments arising from MMP-9 cleavage retain the potential to aggregate and cause toxicity, and whether overexpressing MMP-9 in amyloid-prone islets reduces amyloid burden and the resulting β-cell toxicity. Synthetic hIAPP was incubated with MMP-9 and the major hIAPP fragments observed by MS comprised residues 1–15, 1–25, 16–37, 16–25, and 26–37. The fragments 1–15, 1–25, and 26–37 did not form amyloid fibrils *in vitro* and they were not cytotoxic when incubated with β cells. Mixtures of these fragments with full-length hIAPP did not modulate the kinetics of fibril formation by full-length hIAPP. In contrast, the 16–37 fragment formed fibrils more rapidly than full-length hIAPP but was less cytotoxic. Co-incubation of MMP-9 and fragment 16–37 ablated amyloidogenicity, suggesting that MMP-9 cleaves hIAPP 16–37 into non-amyloidogenic fragments. Consistent with MMP-9 cleavage resulting in largely non-amyloidogenic degradation products, adenoviral overexpression of MMP-9 in amyloid-prone islets reduced amyloid deposition and β-cell apoptosis. These findings suggest that increasing islet MMP-9 activity might be a strategy to limit β-cell loss in type 2 diabetes.

Amyloid deposits are found in the islets of most patients with type 2 diabetes (1), with the degree of deposition being inversely associated with both β-cell mass and function (2, 3). Further, amyloid deposition following islet transplantation is associated with graft failure (4–6). The 37 amino acid peptide constituent of these amyloid deposits, human islet amyloid polypeptide (hIAPP,[5] also known as amylin) is co-secreted with insulin by the β cell (7) and has been shown to be toxic to β cells in culture (8). Thus, reducing amyloid burden to improve β-cell survival has been the focus of a number of studies using different approaches.

Several natural products and small molecule inhibitors of hIAPP-derived amyloid formation have been investigated, as have protein and polypeptide-based inhibitors (reviewed in Ref. 9). However, the therapeutic potential of many of these molecules has not been delineated as some of these studies were carried out in cell-free systems. In addition, many of these compounds are not drug-like; they are chemically labile polyphenols, compounds which are expected to have poor bioavailability or large polypeptides, some of which contain non-genetically coded amino acids. A second approach to limit the deleterious consequences of amyloid deposition is to exploit enzymes that are capable of degrading hIAPP, such as neprilysin and insulin-degrading enzyme (IDE). We and others have shown that up-regulation of neprilysin in hIAPP transgenic mouse islets reduces amyloid deposition and β-cell apoptosis, while its inhibition increases amyloid deposition and β-cell loss (10, 11). Similarly, inhibition of IDE results in increased amyloidogenesis in β-cell lines and reduced cell viability when cells are incubated with synthetic hIAPP (12).

Matrix metalloproteinases (MMPs) are proteolytic enzymes that are involved in the breakdown of extracellular matrix proteins (13). We recently demonstrated that two members of the MMP family, MMP-2 and MMP-9 (also known as gelatinase A

* This work was supported by the Dept. of Veterans Affairs Grant BX001060, NIH Grants DK-007247, DK-017047, DK-020595, DK-080945, DK-088082, DK-098506, GM-078114, and HL-007028. The authors declare that they have no conflict of interest with the contents of this article. The content is solely the responsibility of the authors and does not necessarily represent the official views of the National Institutes of Health.
[1] These authors contributed equally to this work.
[2] Supported by a Swiss National Foundation Fellowship and the Dick and Julia McAbee Endowed Fellowship in Diabetes from the University of Washington.
[3] Supported by an American Diabetes Association Mentor-based Fellowship.
[4] To whom correspondence should be addressed: Steven E. Kahn, VA Puget Sound Health Care System (151), 1660 S. Columbian Way, Seattle, WA. Tel.: 206-277-5515; Fax: 206-764-2164; E-mail: skahn@uw.edu.

[5] The abbreviations used are: hIAPP, human islet amyloid polypeptide; CD, circular dichroism; Fmoc, fluorenylmethoxycarbonyl; HFIP, hexafluoroisopropanol; IDE, insulin-degrading enzyme; MMP, matrix metalloproteinase; rIAPP, rodent islet amyloid polypeptide; TEM, transmission EM; *p*-cyanoPhe, *p*-cyanophenylalanine.

and B) cleave hIAPP (14). Inhibition of MMP-9, but not MMP-2, increased amyloid deposition and β-cell apoptosis in mouse islets, suggesting that MMP-9 plays a physiological role in limiting islet amyloid deposition (14). Further, MMP-9 expression was found to be reduced in islets of subjects with type 2 diabetes (14), suggesting that deficiency of this protease in islets could predispose toward amyloid deposition in humans.

hIAPP is secreted from the β cell and aggregates to form amyloid extracellularly (15). As MMP-9 is localized to the extracellular space (16), this makes it a prime candidate to degrade hIAPP *in vivo*. However, sequence differences exist between species that render some forms of IAPP incapable of aggregating. In particular hIAPP, but not rodent IAPP (rIAPP), is amyloidogenic and cytotoxic (17). These two polypeptides differ at six residues, five of which are located within amino acids 20 through 29. Additional studies using targeted mutations have established that the sequence in this region is an important determinant of the molecule's amyloidogenicity (17–20). hIAPP contains two potential MMP-9 cleavage sites, one between amino acids 15 and 16 and another between amino acids 25 and 26 (14). Cleavage at the latter position should yield fragments with reduced amyloidogenicity and sequential cleavage between amino acids 15 and 16 followed by cleavage between amino acids 25 and 26 would be predicted to also be anti-amyloidogenic. Thus, we sought to investigate the amyloidogenic and cytotoxic potential of MMP-9-cleaved hIAPP fragments. Given that MMP-9 expression is reduced in type 2 diabetes, we also tested whether up-regulation of MMP-9 activity in primary islets can protect from amyloid-induced toxicity.

Experimental Procedures

Peptide Synthesis and Purification—IAPP peptides were synthesized on a 0.25 mmol scale using a microwave peptide synthesizer, by 9-fluorenylmethoxycarbonyl (Fmoc) chemistry as previously described (21). Fmoc-protected pseudoproline dipeptide derivatives were incorporated at positions 9–10, 19–20, and 27–28 to facilitate the synthesis of full-length hIAPP and of a variant containing the fluorescent amino acid *p*-cyanophenylalanine (*p*-cyanoPhe). 5-(4′-Fmoc-aminomethyl-3′, 5-dimethoxyphenol) valeric acid resin was used to generate an amidated C terminus for full-length hIAPP and the fragments 16–37 and 26–37. Fmoc-Phe-PEG-PS resin and Fmoc-Ala-PEG-PS resin were used to form a free C terminus for fragment 1–15 and fragment 1–25, respectively. The disulfide bond was formed via oxidation by DMSO (22). The peptides were purified by reverse-phase HPLC. The identity of the pure products was confirmed by MS using a Bruker MALDI-TOF MS: full-length hIAPP, expected 3903.3, observed 3902.1; fragment 1–15, expected 1639.9, observed 1639.9; fragment 16–37, expected 2282.5, observed 2283.3; fragment 1–25, expected 2667.0, observed 2667.1; fragment 26–37, expected 1254.4, observed 1254.2; hIAPP-F15 *p*-cyanoPhe, expected 3928.3, observed 3928.8.

Sample Preparation—A 1.6 mM peptide solution was prepared in 100% hexafluoroisopropanol (HFIP) and stored at −20 °C. Filtered aliquots were lyophilized for 24 h and resuspended in Tris-HCl buffer (20 mM, pH 7.4).

Thioflavin-T and p-CyanoPhe Fluorescence Assays—Solutions were prepared by adding thioflavin-T (20 mM, in 20 mM Tris-HCl buffer, pH 7.4) to lyophilized peptides. Fluorescence experiments were performed on a Beckman Coulter DTX880 plate reader. An excitation wavelength of 450 nm and emission wavelength of 485 nm was used for these thioflavin-T experiments.

hIAPP-F15 *p*-cyanoPhe is a variant of full-length hIAPP in which the phenylalanine at position 15 was replaced with the non-genetically coded amino acid *p*-cyanophenylalanine. The fluorescence of *p*-cyanoPhe is sensitive to environmental changes and can be used to monitor the kinetics of fibril formation. This substitution does not perturb the kinetics of amyloid formation and the measured time course of fibril formation is identical to the one probed using wild-type hIAPP (23, 24). hIAPP-F15 *p*-cyanoPhe can therefore be used to monitor fibril formation by full-length hIAPP in the presence of another amyloid forming peptide (*e.g.* MMP-9-cleaved hIAPP fragments). Since the fluorescence of *p*-cyanoPhe is high when the cyano group is hydrogen bonded to water (25), the fluorescence signal decreases when hIAPP-F15 *p*-cyanoPhe aggregates. *p*-cyanoPhe flurorescence was excited at 240 nm, and emission was monitored at 296 nm.

Transmission EM (TEM)—At the end of the kinetic reactions, 4 μl of the peptide solution was removed and blotted on a carbon-coated Formvar 300-mesh copper grid for 1 min and then negatively stained with saturated uranyl acetate for 1 min.

Circular Dichroism (CD)—CD experiments were performed using an Applied Photophysics Chirascan CD spectrometer. Spectra were recorded from 190 to 260 nm at 1 nm intervals in a quartz cuvette with 0.1 cm path length at 25 °C. Spectra were background subtracted and presented as unsmoothed curves. CD spectra were measured from aliquots removed at the end of the kinetic (thioflavin-T) experiments.

MALDI-TOF and LC-MS—Unless otherwise specified, 10 μM full-length hIAPP was incubated with or without 0.2 μM recombinant human MMP-9 (EMD, Billerica, MA) at 37 °C for 22 h. Samples were desalted using C18 ZipTips (EMD) and analyzed with MALDI-TOF MS with α-cyano-4-hydroxycinnamic acid as the matrix. For the hIAPP/MMP-9 time course analysis, 10 μM full-length hIAPP was incubated with 0.2 μM MMP-9 and a sample was analyzed by LC/MS after the indicated incubation time. The raw intensity of each peak was normalized to its extinction coefficient.

Cell Line Experiments—The β cell line INS-1 was cultured in RPMI 1640 medium containing 10% fetal bovine serum, 1 mM sodium pyruvate, 100 units/ml penicillin, 100 μg/ml streptomycin, and 11.1 mM glucose (complete medium). 8×10^4 cells/well were plated into a gelatin-coated 96-well plate and incubated for 24 h, after which the medium was replaced with complete medium containing freshly dissolved peptides. After a 24 h incubation, 50 μl of XTT reagent (26) (Roche Applied Science, Madison, WI) was added, and 24 h later absorbance at 492 nm with a reference wavelength of 650 nm was measured. The absorbance of a blank sample (no cells) was used to determine the assay background and was subtracted from every experimental sample. Non-amyloidogenic rIAPP was used as a

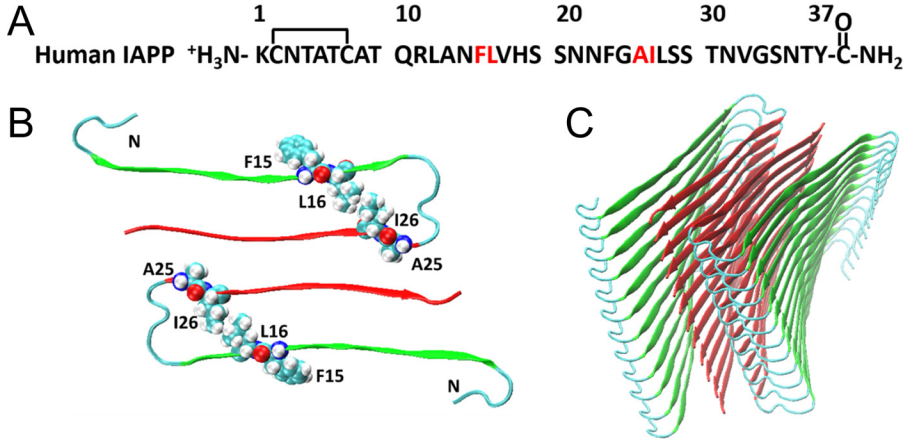

FIGURE 1. **A model of the structure of hIAPP showing potential MMP-9 cleavage sites.** *A*, primary sequence of hIAPP with the MMP-9 cleavage sites 15/16 and 25/26 highlighted in *red*. *B*, top down view of a model of hIAPP amyloid fibrils with Phe-15, Leu-16, Ala-25, and Ile-26 shown in space-filling format. *C*, side view, in *ribbon format*, of the hIAPP structure. The N-terminal β-strand in each monomer is color-coded *red*, the C-terminal β-strand *green*, while the disordered N-terminal region, and the loop that connects the two β-strands are color-coded *blue*.

negative control. Each sample was run in triplicate and normalized to buffer-treated cells.

Primary β-Cell Experiments—Islets from non-transgenic mice were isolated by collagenase digestion and dispersed into single cells (ZymeFreeTM Enzyme Free Cell Dissociation Reagent, VWR, Radnor, PA). Islet cells were then incubated with anti-CD31-FITC antibody (ab33858, Abcam, Cambridge, MA) to label endothelial cells and sorted into a β-cell enriched ("β cell") and a β-cell depleted ("non-β cell") population based on the cell's auto-fluorescence (FACSARIA, BD Biosciences, San Jose, CA). A sample from each population was used for RNA analysis (TaqMan, Applied Biosystems, Carlsbad, CA). 18S was used as housekeeping gene. 1×10^5 cells/well were plated into a 96-well plate, and freshly dissolved peptides added 24 h later. Viability was assessed 24 h later using the XTT assay as described above.

Islet Experiments—Islets from 10 week old transgenic mice with β-cell expression of hIAPP (27) on a F1 C57BL/6 x DBA/2 background and their littermate non-transgenic controls were isolated by collagenase digestion, purified, and transduced with adenoviruses expressing luciferase or human MMP-9 (28) for 24 h (multiplicity of infection = 50, given that an average islet contains 1000 cells) in complete medium. Thereafter, islets were transferred into complete medium containing 16.7 mM glucose and cultured for 144 h with medium being renewed every 48 h. Histological samples were prepared as described elsewhere (29). Briefly, islets were formalin-fixed, paraffin-embedded, sectioned and labeled with thioflavin-S to visualize amyloid deposits and insulin antibody to visualize β cells. Total islet, amyloid, and β-cell areas were calculated from at least 30 islets using a computer-based quantitative method (29). β-cell apoptosis was determined on at least 40 islets by insulin and propidium iodide staining (29). The observer was blinded to the genotype and culture condition of the islets. These studies were approved by the VA Puget Sound Health Care System Institutional Animal Care and Use Committee in Seattle.

MMP-9 Activity—Human MMP-9 activity was measured in islet supernatants collected 144 h after transduction according to the manufacturer's instructions (Human Active MMP-9 Fluorokine E Kit, R&D Systems, Minneapolis, MN).

Statistical Analysis—Data are presented as mean ± S.E. for the number of experiments indicated. Statistical significance was determined using ANOVA with Tukey's Multiple Comparison Test as the post-hoc test or a paired *t* test when only two groups were compared (GraphPad Software, San Diego, CA). To compare the dose responses of full-length hIAPP and hIAPP 16–37, the slope of the linear regression of each experiment was calculated and compared between the two groups using the Mann-Whitney U non-parametric test. A $p < 0.05$ was considered statistically significant.

Results

Human MMP-9 Degrades Monomeric but Not Aggregated hIAPP—The primary sequence of hIAPP includes two likely MMP-9 cleavage sites: the Phe-15-Leu-16 peptide bond and the Ala-25-Ile-26 bond (Fig. 1*A*). A model of the structure of the hIAPP amyloid fibril is displayed in Fig. 1 and is based on crystallographic studies of small fragments of hIAPP (30).

To test the susceptibility of monomeric hIAPP and aggregated hIAPP fibrils to cleavage by MMP-9, freshly dissolved full-length hIAPP was incubated with MMP-9 or buffer and analyzed by TEM and MS 22 h later. A dense mesh of fibrils was evident in the buffer-treated sample (Fig. 2*A*). In contrast, when full-length hIAPP was incubated with MMP-9, TEM showed the existence of only a few aggregates (Fig. 2*B*) and MS detected products consistent with MMP-9 cleavage of hIAPP between residues 15 and 16 as well as between residues 25 and 26 (Fig. 2*C*).

We next tested whether MMP-9 is able to cleave pre-aggregated hIAPP fibrils. For this experiment, full-length hIAPP was aggregated for 24 h, a time which is longer than required to form amyloid fibrils, MMP-9 was added and a sample removed for analysis 24 h later. TEM of buffer or MMP-9-treated samples were indistinguishable and both revealed dense mats of amyloid fibrils (Fig. 2, *D* and *E*). No degradation products were detected by MS following incubation of aggregated full-length hIAPP with MMP-9 (Fig. 2*F*).

Identification and Time-dependent Abundance of MMP-9-cleaved hIAPP Degradation Products—Incubation of full-length hIAPP with MMP-9 and subsequent analysis of the degradation products by LC/MS as a function of time confirmed

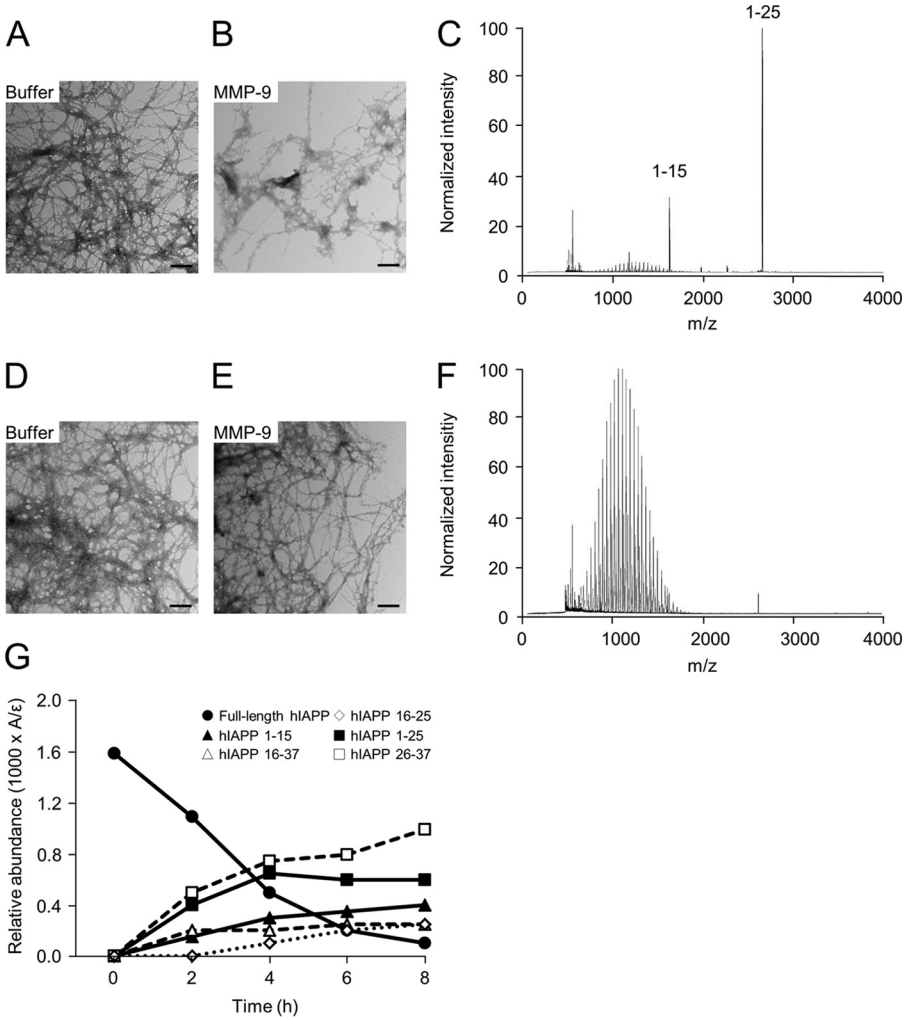

FIGURE 2. **MMP-9 degrades monomeric hIAPP but not hIAPP fibrils, and this degradation is time dependent.** 10 μM full-length hIAPP and 0.2 μM MMP-9 were combined at the beginning (*A* and *B*) or after 24 h of hIAPP pre-incubation (*D* and *E*) when the aggregation kinetic reached a plateau. Samples for TEM were removed 24 h later. MS of samples that had been mixed with MMP-9 at the beginning (*C*) or at 24 h (*F*) of the experiment are shown. The prominent signal in the mass spectra at ~500–1500 *m/z* originates from the matrix and is therefore considered background. Scale bar represents 200 nm. *G*, abundance of full-length hIAPP, hIAPP 1–15, hIAPP 16–37, hIAPP 1–25, hIAPP 26–37, and hIAPP 16–25 measured by LC/MS 0, 2, 4, 6, and 8 h after combining 10 μM full-length hIAPP with 0.2 μM MMP-9.

that MMP-9 cleaves between residues 15 and 16 as well as 25 and 26 (Fig. 2*G*). All four fragments yielded by a single cleavage (1–15, 16–37, 1–25, and 26–37) were detected early on and their relative amount remained constant over time, except for hIAPP 26–37 whose amount increased over the course of the experiment. In contrast, the amount of full-length hIAPP decreased over time, as expected, and was barely detectable at 8 h. hIAPP 16–25 was not detected at 2 h but appeared at 4 h and increased thereafter, consistent with it being the only product resulting from two distinct cleavages.

hIAPP 16–37 Readily Aggregates into Amyloid Fibrils and Can Be Cleaved Further by MMP-9—We synthesized full-length hIAPP as well as the degradation products hIAPP 1–15, 16–37, 1–25, and 26–37 and tested their ability to form amyloid fibrils using thioflavin-T binding assays and TEM. As expected, the kinetic curve observed for full-length hIAPP exhibited a distinct lag phase on the order of 15 h followed by a growth phase until the final plateau was reached (Fig. 3*A*). TEM images collected at the end of the reaction revealed a dense mat of amyloid fibrils (Fig. 3*C*) and CD spectra indicated the presence of β-sheets (Fig. 3*D*). In contrast, hIAPP 1–15, 1–25, and 26–37 did not exhibit any increase in thioflavin-T fluorescence over the entire time course of the study (Fig. 3*A*), even when these fragments were incubated in the presence of 20% glycerol (Fig. 3*B*) or 2% HFIP (data not shown), both conditions known to promote amyloid formation. The absence of fibrils was confirmed by TEM (Fig. 3*C*), and CD spectra showed that hIAPP 1–15, 1–25 and 26–37 remained in random coil confirmation (Fig. 3*D*). In contrast to the other fragments, thioflavin-T fluorescence of hIAPP 16–37 increased rapidly without an initial lag phase leading to a maximal signal, which was similar to that of full-length hIAPP (Fig. 3*A*). TEM and CD showed that hIAPP 16–37 forms fibrils (Fig. 3*C*) and adopts a β-sheet structure (Fig. 3*D*).

Since hIAPP 16–37 possesses a potential MMP-9 cleavage site between residues 25 and 26, we investigated whether MMP-9 has the ability to further cleave hIAPP 16–37 into smaller potentially non-amyloidogenic fragments. Thioflavin-T fluorescence over time (Fig. 3*E*) and TEM images taken at the end of the experiment (Fig. 3*F*) demonstrated that incubation with MMP-9 abolished fibril formation by hIAPP 16–37.

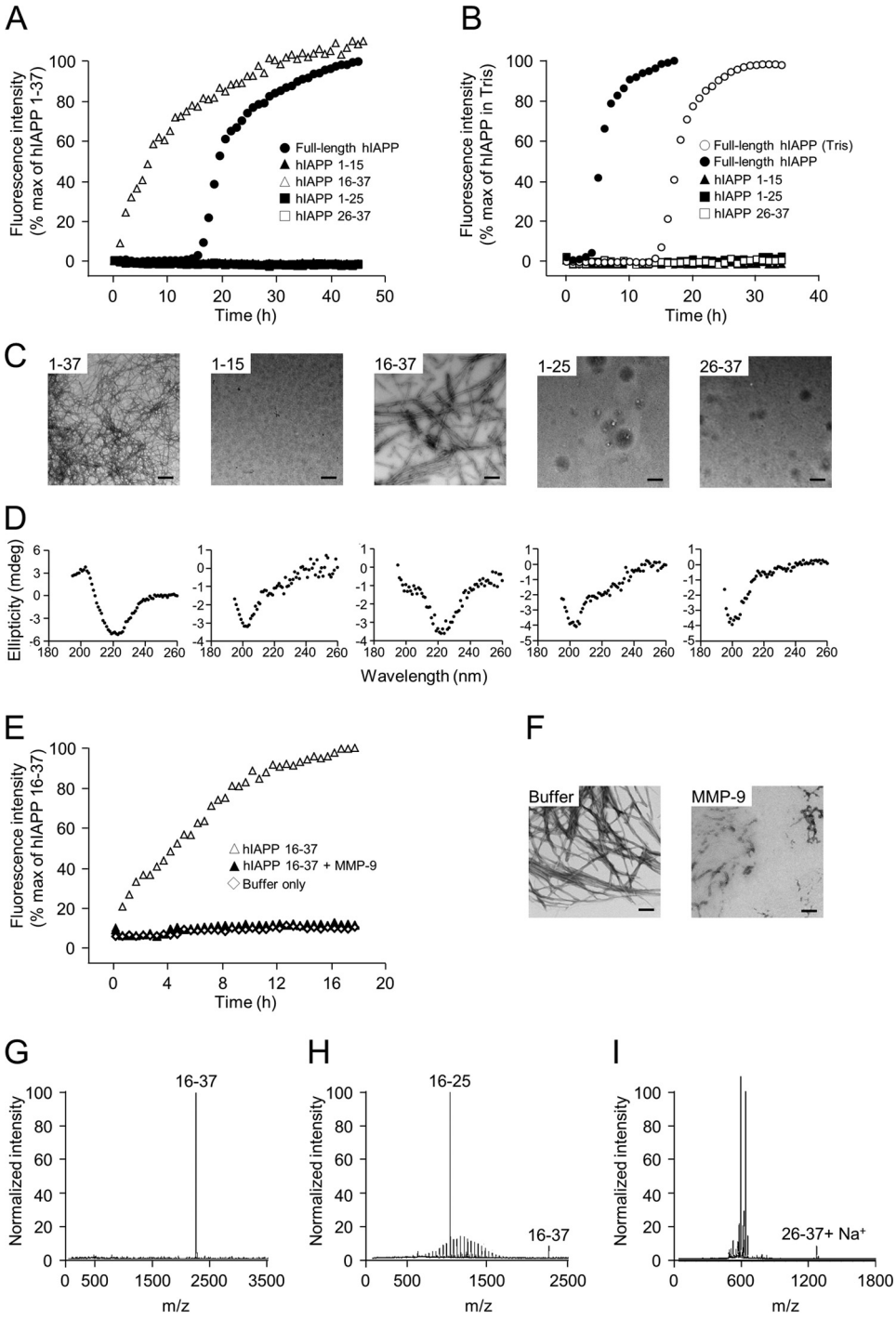

FIGURE 3. **hIAPP 16–37 readily aggregates into amyloid fibrils, and can be cleaved further by MMP-9.** Thioflavin-T fluorescence kinetics of full-length hIAPP, hIAPP 1–15, hIAPP 16–37, hIAPP 1–25, and hIAPP 26–37 in Tris buffer (*A*) and 20% glycerol (*B*). The corresponding TEMs (*C*) and CD spectra (*D*) in Tris buffer are shown. hIAPP 1–15, hIAPP 1–25, and hIAPP 26–37 are overlapping and do not exhibit an increase in fluorescence. Peptide concentrations were 16 μM. Thioflavin-T fluorescence kinetics (*E*) and TEMs (*F*) of hIAPP 16–37, hIAPP 16–37 + MMP-9 and buffer only. hIAPP 16–37 + MMP-9 and buffer only are overlapping. Note that the kinetic is accelerated compared with Fig. 3*A* due to the MMP-9 buffer containing 20% glycerol. MS of hIAPP 16–37 (*G*) and hIAPP 16–37 plus MMP-9 (*H*) are depicted. hIAPP 26–37 is difficult to detect by mass spectrometry as shown by MS of hIAPP 26–37 showing a weak signal at the expected mass for hIAPP 26–37 (1254.4 *m*/*z*) (*I*). TEM and MS samples were taken at the end of the kinetic reactions. The peptide concentrations were 10 μM, and the concentration of MMP-9 was 0.2 μM. Scale bar represents 200 nm. Representative images of $n = 3$ experiments are shown.

In addition, disappearance of hIAPP 16–37 and subsequent appearance of hIAPP 16–25 following MMP-9 treatment was shown by MS (Fig. 3, *G* and *H*). Since hIAPP 26–37 was not detected by MS following MMP-9 degradation of full-length hIAPP (Fig. 2*C*) or hIAPP 16–37 (Fig. 3*H*), we analyzed synthetic hIAPP 26–37 and found that it does not ionize efficiently enough to be readily detected by MS (Fig. 3*I*).

Non-Amyloidogenic hIAPP Fragments Are Not Cytotoxic and hIAPP 16–37 Is Less Cytotoxic Than Full-length hIAPP—We next determined whether the hIAPP fragments produced by

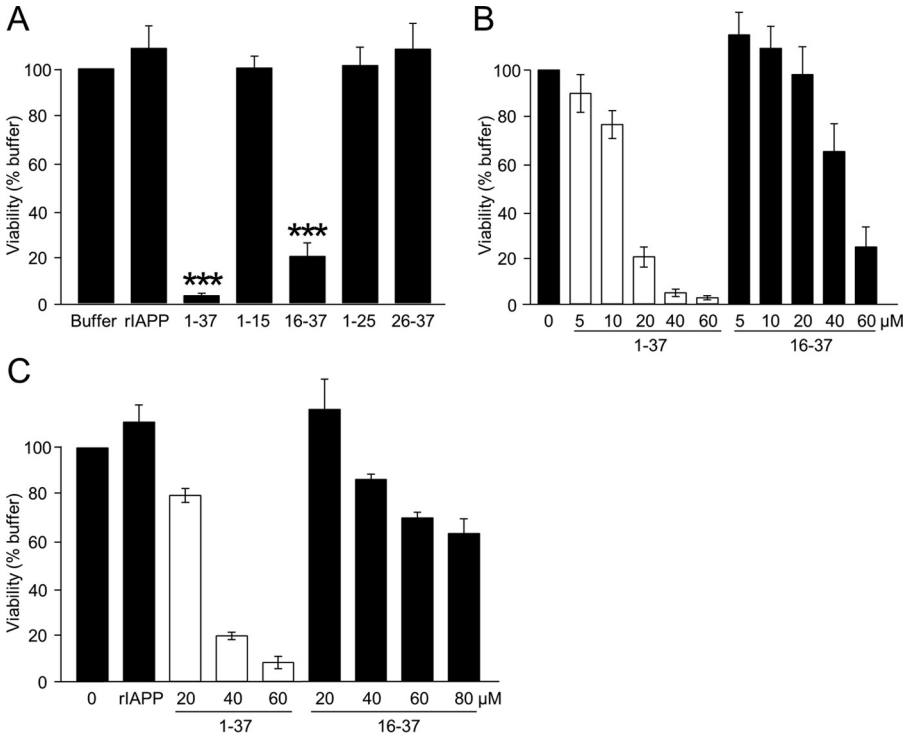

FIGURE 4. **Non-amyloidogenic hIAPP fragments are not cytotoxic and hIAPP 16–37 is less cytotoxic than full-length hIAPP.** *A*, viability of INS-1 cells 24 h after exposure to 60 μM of the indicated hIAPP fragments ($n = 4$). *B*, indicated concentrations of full-length hIAPP or hIAPP 16–37 were added to INS-1 cells and cell viability was measured 24 h later ($n = 7$). *C*, viability of primary mouse β cells 24 h after exposure to the indicated concentrations of hIAPP peptides ($n = 4$). The arbitrary value of the buffer control in each experiment was set to 100. The non-amyloidogenic rIAPP was included as a negative control. ***, $p < 0.001$ *versus* buffer control.

MMP-9 cleavage are cytotoxic. Full-length hIAPP is known to be cytotoxic (8) and was used as a positive control, while non-toxic rIAPP (17) was used as negative control. Viability of INS-1 β cells following 24 h exposure to 60 μM of the hIAPP fragments 1–15, 1–25 and 26–37 was indistinguishable from cells treated with either buffer alone or 60 μM rIAPP (Fig. 4*A*). In contrast, hIAPP fragment 16–37 was cytotoxic, but appeared less cytotoxic than full-length hIAPP at this same dose.

To directly compare the cytotoxic potential of hIAPP 16–37 and full-length hIAPP, the dose-response curve of both peptides was determined in INS-1 β cells. While 10 μM full-length hIAPP reduced cell viability to 77 $\pm$ 6% of buffer control, only doses at or above 40 μM hIAPP 16–37 significantly reduced viability (40 μM: 65 $\pm$ 12%; Fig. 4*B*). Regression coefficient analysis revealed that hIAPP 16–37 was less cytotoxic than full-length hIAPP (slope hIAPP 1–37: -1.89 ± 0.16; slope hIAPP 16–37: -1.16 ± 0.24; $p < 0.05$).

We also tested the potential of hIAPP 16–37 to induce toxicity in primary β cells. For this, mouse islet cells were sorted into a β-cell and a non-β-cell fraction, with RNA analysis showing an enrichment of β-cell specific genes and a reduction of α- and δ-cell specific genes in the β-cell fraction relative to the non-β-cell fraction (increased: insulin 2: $+55.9 \pm 12.1$-fold; IAPP: $+5.7 \pm 1.0$-fold; decreased: glucagon: -3.5 ± 1.1-fold; somatostatin: -4.3 ± 1.7-fold). hIAPP 16–37 reduced viability in primary β cells in a dose-dependent manner, but this was again less than that observed with full-length hIAPP (slope hIAPP 1–37: -1.68 ± 0.04; slope hIAPP 16–37: -0.595 ± 0.04; $p < 0.05$; Fig. 4*C*).

hIAPP 16–37 Accelerates Amyloid Formation by Full-Length hIAPP, But the Other hIAPP Fragments Do Not—Some hIAPP-derived fragments and structurally related peptides have been shown to be able to inhibit while others have been shown to be able to enhance fibril formation (31–34). To test whether hIAPP 16–37 is able to modulate the aggregation kinetics of full-length hIAPP, mixtures of full-length hIAPP and hIAPP 16–37 at ratios of 1:0.5, 1:1, 1:5, and 1:10 were analyzed. hIAPP 16–37 accelerated fibril formation by full-length hIAPP in a dose-dependent manner (Fig. 5*A*). The maximal fluorescence was increased and T50, the time to reach 50% of the maximal fluorescence signal, was reduced in a dose-dependent manner (Fig. 5*B*). Since the thioflavin-T fluorescent signal does not discern between fibrils derived from full-length hIAPP or hIAPP 16–37, we used the fluorescent hIAPP-F15 *p*-cyanoPhe analog to monitor fibril formation by full-length hIAPP, independent of any contribution of hIAPP 16–37 to the total fibril formation. Addition of a 5-fold excess of hIAPP 16–37 accelerated hIAPP-F15 *p*-cyanoPhe fibril formation and a much shorter lag phase was observed (Fig. 5*C*).

The other non-amyloidogenic fragments were also tested for their effect on amyloid formation by measuring the resulting thioflavin-T kinetics and by obtaining TEM images of the mixtures. Addition of hIAPP 1–15 (Fig. 6*A*), hIAPP 1–25 (Fig. 6*B*) or hIAPP 26–37 (Fig. 6*C*) to full-length hIAPP did not alter thioflavin-T kinetics at any of the ratios tested. TEMs obtained at the end of the kinetic analysis confirmed the finding that fibril formation was not inhibited (Fig. 6*D*). T50 was slightly greater with the mixtures of 1:1 and 1:5 full-length hIAPP to

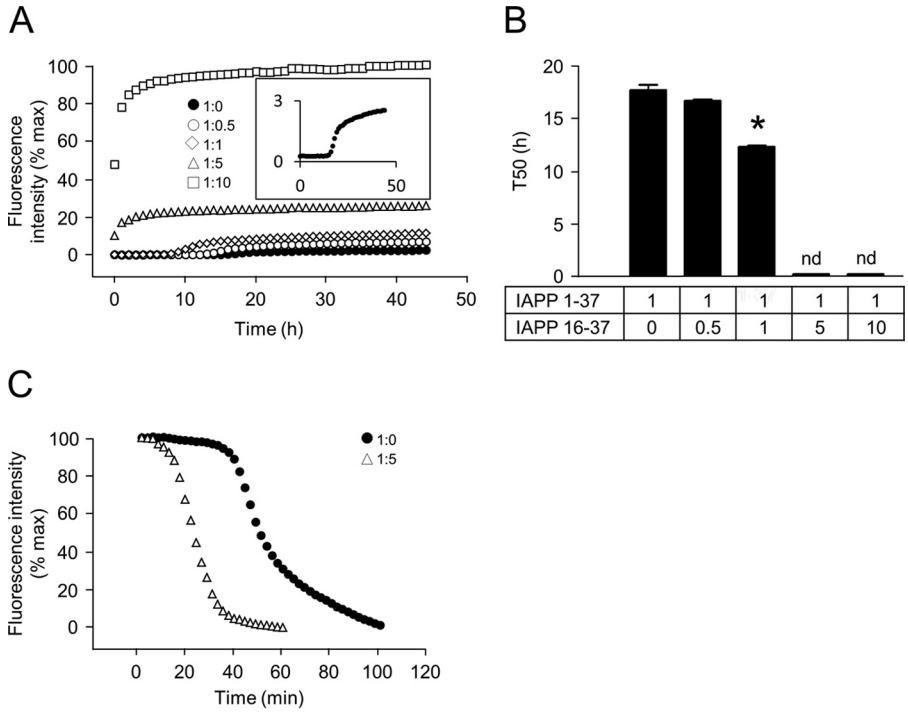

FIGURE 5. **hIAPP 16–37 accelerates amyloid formation by full-length hIAPP.** *A*, thioflavin-T fluorescence kinetics are shown for 16 μM full-length hIAPP alone or 16 μM full-length hIAPP with the addition of hIAPP 16–37 at ratios of 1:0.5, 1:1, 1:5, and 1:10. To show that the aggregation kinetic of full-length hIAPP alone has the expected sigmoidal shape, the kinetic of full-length hIAPP is reproduced on a different axis in the *inset* ($n = 3$). *B*, T50 (time to reach 50% maximal fluorescence) for the kinetic curves in *A* was calculated and is shown for the indicated peptide ratios. Note that the aggregation with 5- and 10-fold excess of hIAPP 16–37 was too fast to accurately measure T50. *, $p < 0.05$ *versus* full-length hIAPP alone ($n = 3$). *C*, fluorescence kinetics of 16 μM full-length *p*-cyanoPhe-hIAPP with or without 5-fold excess hIAPP 16–37 are shown. Note *p*-cyanoPhe fluorescence decreases with increased peptide aggregation as the quantum yield is lower in the aggregated state ($n = 2$).

hIAPP 1–25, but was not different with the other peptide ratios (Fig. 6*E*). Further, T50 was not altered when hIAPP 1–15 or 26–37 were mixed with full-length hIAPP (Fig. 6*E*).

hIAPP 1–15 Does Not Potently Inhibit Amyloid Formation by hIAPP 16–37—Given that hIAPP 16–37 lacks the initial lag phase and rapidly aggregates into amyloid fibrils, we tested if addition of hIAPP 1–15 inhibited amyloid formation by hIAPP 16–37. Indeed, thioflavin-T kinetics of a 1:1 mixture of hIAPP 16–37 and 1–15 suggested that the aggregation of hIAPP 16–37 was somewhat reduced in the presence of hIAPP 1–15 (data now shown). Consequently, we further tested the potential of hIAPP 1–15 to inhibit aggregation of hIAPP 16–37, but even a 10-fold excess of hIAPP 1–15 did not further inhibit aggregation of hIAPP 16–37 (Fig. 6*F*).

MMP-9 Overexpression Reduces Amyloid-induced β-Cell Apoptosis in Mouse Islets—Since the MMP-9 cleavage products, with the exception of hIAPP 16–37, are not toxic and the latter is less toxic than full-length hIAPP, and is further cleaved into non-toxic fragments by MMP-9, we hypothesized that up-regulation of human MMP-9 activity in islets protects against amyloid formation and the resulting β-cell toxicity. Amyloid-prone hIAPP transgenic mouse islets were transduced and cultured at 16.7 mM glucose to induce amyloid deposition and β-cell apoptosis (35, 36). MMP-9-transduction increased human MMP-9 activity in islet supernatants (Fig. 7*A*). As expected, non-transgenic mouse islets did not develop amyloid deposits, while hIAPP transgenic islets contained amyloid (Fig. 7*B*). MMP-9 overexpression significantly reduced amyloid deposition in hIAPP transgenic mouse islets (Fig. 7*B*). Finally, the number of apoptotic β-cells was increased 5-fold in amyloid-containing islets compared with non-transgenic control islets. MMP-9 overexpression did not significantly change the rate of β-cell apoptosis in non-transgenic islets but reduced amyloid-induced β-cell apoptosis in hIAPP transgenic islets by 47% (Fig. 7*C*).

Discussion

The data presented here demonstrate that MMP-9 decreases amyloid formation in cell-free systems and cultured, isolated islets. With the exception of the 16–37 fragment, the MMP-9 cleavage products of hIAPP are neither amyloidogenic nor toxic to β cells. hIAPP 16–37 is toxic, but is significantly less so than full-length hIAPP. In addition, hIAPP 16–37 itself is further cleaved into non-amyloidogenic fragments by MMP-9. Further, MMP-9 overexpression reduces amyloid deposition and amyloid-induced β-cell apoptosis in isolated mouse islets. Thus, up-regulation of MMP-9 might be a valid strategy to protect human islets from amyloid-induced damage.

The unique peptide constituent of the islet amyloid deposits observed in humans with type 2 diabetes is the β cell secretory product hIAPP. hIAPP is known to be secreted into the extracellular space (15) where MMP-9 is present (16). Thus, MMP-9 is ideally positioned to degrade hIAPP and limit fibril formation. We have previously reported that inhibition of MMP-9 protease activity increases amyloid deposition and amyloid-induced β-cell apoptosis in isolated hIAPP transgenic mouse islets (14), suggesting that MMP-9 is part of a physiological clearance mechanism that protects the islet from excess hIAPP.

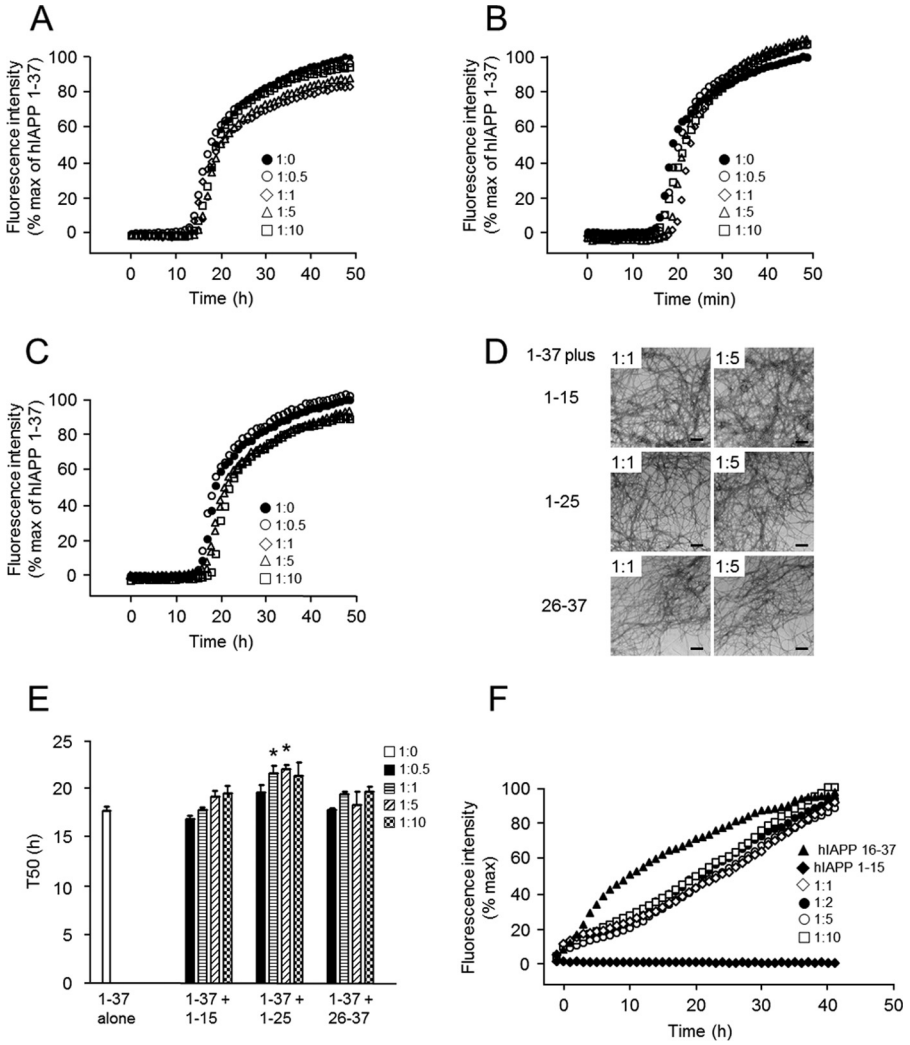

FIGURE 6. **hIAPP fragments do not inhibit amyloid formation by full-length hIAPP.** Thioflavin-T fluorescence kinetics are shown for 16 μM full-length hIAPP with or without hIAPP fragments at ratios of 1:0.5, 1:1, 1:5, and 1:10. Representative fluorescence profiles of the three non-amyloidogenic peptides hIAPP 1–15 (*A*), hIAPP 1–25 (*B*), and hIAPP 26–37 (*C*) are shown. TEMs from samples removed at the end of the kinetics are shown in *D*. Scale bar represents 200 nm. T50 (time to reach 50% maximal fluorescence) was calculated and is presented in *E*. *, $p < 0.05$ *versus* full-length hIAPP alone ($n = 3$). *F*, thioflavin-T fluorescence kinetics are shown for 16 μM hIAPP 16–37 alone or 16 μM hIAPP 16–37 with the addition of hIAPP 1–15 at ratios of 1:1, 1:2, 1:5, and 1:10. 16 μM hIAPP 1–15 alone is shown as control ($n = 3$).

Islet amyloid deposits are present in the majority of patients with type 2 diabetes (3) and interestingly, we found reduced MMP-9 expression levels in islets from patients with type 2 diabetes (14). These data suggest that under physiological conditions MMP-9 acts to reduce amyloid accumulation and that this clearance mechanism is likely to be dysfunctional in humans with type 2 diabetes.

Our data show that MMP-9 is able to degrade monomeric hIAPP, but not aggregated hIAPP fibrils. A possible explanation for this is that MMP-9 can bind monomeric hIAPP but not hIAPP in amyloid deposits. This is supported by two high resolution structure models of hIAPP aggregation (30, 37). As depicted in Fig. 1, the model of Wiltzius and colleagues places the MMP-9 cleavage site between residues Phe-15 and Leu-16 in the ordered N-terminal β-strand and residues Ala-25 and Ile-26 in the ordered core on the inside of the fibril. This suggests that, unlike monomeric hIAPP, the aggregated amyloid fibril structure protects the potential cleavage sites from attack by MMP-9. This finding is consistent with another model of hIAPP fibril formation (37), which, in contrast to the first model, places residues 25 and 26 in a partially ordered loop/turn that links the two β-strands, similarly suggesting that hIAPP fibrils are protected from MMP-9 attack.

All but one of the tested MMP-9-cleaved hIAPP fragments did not induce β-cell toxicity *in vitro*. The absence of toxicity is likely explained by the lack of amyloidogenicity of these peptides. Although hIAPP residues 8–20, 10–19, and 30–37 have been shown to have the potential to form amyloid when incubated at high concentrations (38, 39), we found the MMP-9-cleaved hIAPP fragments 1–15, 1–25, and 26–37 did not form amyloid even when they were incubated under conditions that promote amyloid formation. It is likely that the disulfide bond in hIAPP 1–15 and the charged groups at both termini (Lys and Arg) are not compatible with β-sheet structures. Computer algorithms that predict amyloidogenicity and aggregation regions in unfolded polypeptide chains (40, 41) confirm the absence of potential to aggregate in the hIAPP fragments 1–15 and 26–37. The 8–20 fragment of hIAPP can form amyloid in

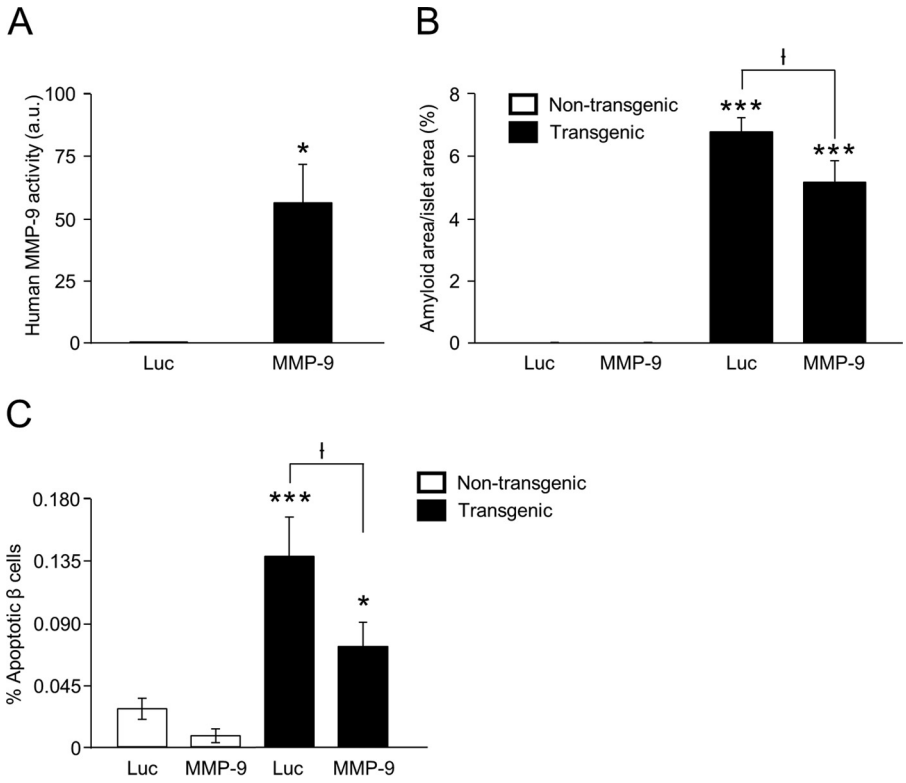

FIGURE 7. **MMP-9 overexpression reduces amyloid deposition and β-cell apoptosis in hIAPP transgenic mouse islets.** Human MMP-9 activity in supernatants of mouse islets transduced with adenoviruses that express luciferase (luc) or MMP-9 is shown in *A*. *, $p < 0.05$ *versus* luc ($n = 3$). Amyloid area/islet area (*B*) and % apoptotic β cells (*C*) of transduced islets are shown. *, $p < 0.05$ and ***, $p < 0.001$ *versus* non-transgenic controls. †, $p < 0.05$ transgenic luciferase *versus* transgenic MMP-9 ($n = 5$).

isolation, but the constraints induced by the disulfide bond and the charged groups at the N terminus and in the middle of the peptide likely overcome the aggregation prone residues 8–20 in hIAPP 1–25. While one of the computer algorithms calculates no amyloidogenicity for hIAPP 1–25, the other predicts a potential aggregation site at residues 12–17, although with much lower aggregation potential than full-length hIAPP. It is of course possible that hIAPP 1–25 forms amyloid if incubated for several days at a high concentration, but these conditions are not relevant to the situation *in vivo*. Thus, consistent with our experimental observations, these computational analysis suggest that hIAPP fragments 1–15, 1–25, and 26–37 have no or very modest potential to aggregate.

We found one of the MMP-9-cleaved hIAPP fragments, namely 16–37, readily forms amyloid fibrils. This fragment contains amino acids 20–29 of the full-length peptide. These ten residues were previously found to influence the potential of full-length hIAPP to aggregate and they were also shown to be able to independently assemble into fibrils (17, 42). Further, hIAPP 16–37 was toxic to β cells (both primary and transformed) and accelerated the aggregation of full-length hIAPP. This suggests that the production of hIAPP 16–37 is associated with a pro-apoptotic phenotype. However, we do not believe that hIAPP 16–37 is a major determinant of amyloid-induced β-cell apoptosis *in vivo*. First, hIAPP 16–37 has an MMP-9 cleavage site between residues 25–26 and co-incubation of hIAPP 16–37 with MMP-9 leads to non-amyloidogenic and non-cytotoxic fragments. Second, it has been speculated that early aggregates (oligomers) of hIAPP are the major cytotoxic species and that fully aggregated hIAPP is inert (43–47). We observed that hIAPP 16–37 aggregates much faster than full-length hIAPP and one could speculate that it therefore reaches the inert aggregated state more quickly. In line with this hypothesis, we found that hIAPP 16–37 was less cytotoxic than full-length hIAPP when cultured with either primary or transformed β cells. A third reason why hIAPP 16–37 probably does not contribute substantially to amyloid formation *in vivo* is that, based on the abundance of the cleavage products, our data suggest that Ala25-Ile26 is MMP-9's preferred cleavage site and that the yield of hIAPP 16–37 *per se* is likely to be rather low. Overall, these data suggest that even though hIAPP 16–37 is cytotoxic, its abundance *in vivo* is probably insignificant and its pro-amyloidogenic/cytotoxic effects negligible.

Hexapeptides derived from the amyloidogenic region 20–29 as well as other hIAPP fragments and structurally related peptides have been shown to be modulators of hIAPP fibrillogenesis (31–34). For MMP-9 cleavage of hIAPP to be a target to reduce amyloid formation and cytotoxicity, it is important that its cleavage products do not aggravate full-length hIAPP's toxicity. Mixtures of full-length hIAPP with up to 10-fold excess hIAPP 1–15, 1–25, or 26–37 did not influence the aggregation kinetics of full-length hIAPP, suggesting that these fragments do not exacerbate amyloid-induced damage.

Finally, we tested these findings from cell-free and *in vitro* systems in primary islets. MMP-9 up-regulation reduced amyloid deposition in isolated islets by 25% and amyloid-induced β-cell apoptosis by 50%. These observations suggest that MMP-9 may have therapeutic potential. First, MMP-9 activa-

tion in the islet could be used to reduce amyloid-induced cytotoxicity in type 2 diabetes. This concept is supported by the fact that islets from patients with type 2 diabetes have reduced MMP-9 expression (14). A second potential area of interest for MMP-9 activation could be islet transplantation where amyloid formation is associated with loss of β cells, transplant failure, and the recurrence of hyperglycemia (4, 5, 48, 49).

In summary, our findings show that MMP-9 cleavage of hIAPP largely ablates hIAPP aggregation and amyloid-induced toxicity. Thus, increasing MMP-9 activity *in vivo* could be a strategy to protect the islet from amyloid-induced damage in human diabetes.

Author Contributions—D. T. M. contributed to the study design, performed research, analyzed data, and wrote the manuscript. L. H. T. contributed to the study design, performed research, analyzed data, and reviewed/edited the manuscript. M. F. H., A. T. T., and R. L. H. helped interpret the data and reviewed/edited the manuscript. S. Z., D. P. R., and S. E. K. contributed to the study design, helped interpret the data and reviewed/edited the manuscript. D. T. M. is the guarantor of this work and, as such, had full access to all the data in the study and takes responsibility for the integrity of the work as a whole.

Acknowledgments—We thank Breanne Barrow, Michael Peters, Bela Ruzsicska, Joshua Willard, Phillip Bergquist, Daryl Hackney, Atiqur Rahman, Jessica Wilkins-Gutierrez, and Chantruyen Ho for excellent technical support, Peter Marek and Amy G. Wong for helpful discussions and experimental assistance and Rehana Akter for help with the structure model figure. The adenoviruses were kindly provided by Jack Gauldie (McMaster University, Hamilton, Ontario) and Christopher J. Rhodes (University of Chicago, Chicago, IL).

References

1. Westermark, P. (1972) Quantitative studies on amyloid in the islets of Langerhans. *Ups. J. Med. Sci.* **77,** 91–94
2. Hull, R. L., Westermark, G. T., Westermark, P., and Kahn, S. E. (2004) Islet amyloid: a critical entity in the pathogenesis of type 2 diabetes. *J. Clin. Endocrinol. Metab.* **89,** 3629–3643
3. Jurgens, C. A., Toukatly, M. N., Fligner, C. L., Udayasankar, J., Subramanian, S. L., Zraika, S., Aston-Mourney, K., Carr, D. B., Westermark, P., Westermark, G. T., Kahn, S. E., and Hull, R. L. (2011) Beta-cell loss and beta-cell apoptosis in human type 2 diabetes are related to islet amyloid deposition. *Am. J. Pathol.* **178,** 2632–2640
4. Westermark, G. T., Westermark, P., Berne, C., Korsgren, O., and Nordic Network for Clinical Islet, T. (2008) Widespread amyloid deposition in transplanted human pancreatic islets. *N. Engl. J. Med.* **359,** 977–979
5. Potter, K. J., Abedini, A., Marek, P., Klimek, A. M., Butterworth, S., Driscoll, M., Baker, R., Nilsson, M. R., Warnock, G. L., Oberholzer, J., Bertera, S., Trucco, M., Korbutt, G. S., Fraser, P. E., Raleigh, D. P., and Verchere, C. B. (2010) Islet amyloid deposition limits the viability of human islet grafts but not porcine islet grafts. *Proc. Natl. Acad. Sci. U.S.A.* **107,** 4305–4310
6. Udayasankar, J., Kodama, K., Hull, R. L., Zraika, S., Aston-Mourney, K., Subramanian, S. L., Tong, J., Faulenbach, M. V., Vidal, J., and Kahn, S. E. (2009) Amyloid formation results in recurrence of hyperglycaemia following transplantation of human IAPP transgenic mouse islets. *Diabetologia* **52,** 145–153
7. Kahn, S. E., D'Alessio, D. A., Schwartz, M. W., Fujimoto, W. Y., Ensinck, J. W., Taborsky, G. J., Jr., and Porte, D., Jr. (1990) Evidence of cosecretion of islet amyloid polypeptide and insulin by beta-cells. *Diabetes* **39,** 634–638
8. Lorenzo, A., Razzaboni, B., Weir, G. C., and Yankner, B. A. (1994) Pancreatic islet cell toxicity of amylin associated with type-2 diabetes mellitus. *Nature* **368,** 756–760
9. Cao, P., Marek, P., Noor, H., Patsalo, V., Tu, L. H., Wang, H., Abedini, A., and Raleigh, D. P. (2013) Islet amyloid: from fundamental biophysics to mechanisms of cytotoxicity. *FEBS Lett.* **587,** 1106–1118
10. Zraika, S., Aston-Mourney, K., Marek, P., Hull, R. L., Green, P. S., Udayasankar, J., Subramanian, S. L., Raleigh, D. P., and Kahn, S. E. (2010) Neprilysin impedes islet amyloid formation by inhibition of fibril formation rather than peptide degradation. *J. Biol. Chem.* **285,** 18177–18183
11. Guan, H., Chow, K. M., Shah, R., Rhodes, C. J., and Hersh, L. B. (2012) Degradation of islet amyloid polypeptide by neprilysin. *Diabetologia* **55,** 2989–2998
12. Bennett, R. G., Hamel, F. G., and Duckworth, W. C. (2003) An insulin-degrading enzyme inhibitor decreases amylin degradation, increases amylin-induced cytotoxicity, and increases amyloid formation in insulinoma cell cultures. *Diabetes* **52,** 2315–2320
13. Chen, Q., Jin, M., Yang, F., Zhu, J., Xiao, Q., and Zhang, L. (2013) Matrix metalloproteinases: inflammatory regulators of cell behaviors in vascular formation and remodeling. *Mediators Inflamm.* **2013,** 928315
14. Aston-Mourney, K., Zraika, S., Udayasankar, J., Subramanian, S. L., Green, P. S., Kahn, S. E., and Hull, R. L. (2013) Matrix metalloproteinase-9 reduces islet amyloid formation by degrading islet amyloid polypeptide. *J. Biol. Chem.* **288,** 3553–3559
15. Verchere, C. B., D'Alessio, D. A., Palmiter, R. D., Weir, G. C., Bonner-Weir, S., Baskin, D. G., and Kahn, S. E. (1996) Islet amyloid formation associated with hyperglycemia in transgenic mice with pancreatic beta cell expression of human islet amyloid polypeptide. *Proc. Natl. Acad. Sci. U.S.A.* **93,** 3492–3496
16. Tomita, T., and Iwata, K. (1997) Gelatinases and inhibitors of gelatinases in pancreatic islets and islet cell tumors. *Mod. Pathol.* **10,** 47–54
17. Westermark, P., Engström, U., Johnson, K. H., Westermark, G. T., and Betsholtz, C. (1990) Islet amyloid polypeptide: pinpointing amino acid residues linked to amyloid fibril formation. *Proc. Natl. Acad. Sci. U.S.A.* **87,** 5036–5040
18. Moriarty, D. F., and Raleigh, D. P. (1999) Effects of sequential proline substitutions on amyloid formation by human amylin20–29. *Biochemistry* **38,** 1811–1818
19. Betsholtz, C., Christmansson, L., Engström, U., Rorsman, F., Svensson, V., Johnson, K. H., and Westermark, P. (1989) Sequence divergence in a specific region of islet amyloid polypeptide (IAPP) explains differences in islet amyloid formation between species. *FEBS Lett.* **251,** 261–264
20. Buchanan, L. E., Dunkelberger, E. B., Tran, H. Q., Cheng, P. N., Chiu, C. C., Cao, P., Raleigh, D. P., de Pablo, J. J., Nowick, J. S., and Zanni, M. T. (2013) Mechanism of IAPP amyloid fibril formation involves an intermediate with a transient beta-sheet. *Proc. Natl. Acad. Sci. U.S.A.* **110,** 19285–19290
21. Marek, P., Woys, A. M., Sutton, K., Zanni, M. T., and Raleigh, D. P. (2010) Efficient microwave-assisted synthesis of human islet amyloid polypeptide designed to facilitate the specific incorporation of labeled amino acids. *Org. Lett.* **12,** 4848–4851
22. Abedini, A., Singh, G., and Raleigh, D. P. (2006) Recovery and purification of highly aggregation-prone disulfide-containing peptides: application to islet amyloid polypeptide. *Anal. Biochem.* **351,** 181–186
23. Marek, P., Mukherjee, S., Zanni, M. T., and Raleigh, D. P. (2010) Residue-Specific, Real-Time Characterization of Lag-Phase Species and Fibril Growth During Amyloid Formation: A Combined Fluorescence and IR Study of p-Cyanophenylalanine Analogs of Islet Amyloid Polypeptide. *J. Mol. Biol.* **400,** 878–888
24. Marek, P., Gupta, R., and Raleigh, D. P. (2008) The fluorescent amino acid p-cyanophenylalanine provides an intrinsic probe of amyloid formation. *Chembiochem* **9,** 1372–1374
25. Tucker, M. J., Oyola, R., and Gai, F. (2006) A novel fluorescent probe for protein binding and folding studies: p-cyano-phenylalanine. *Biopolymers* **83,** 571–576
26. Scudiero, D. A., Shoemaker, R. H., Paull, K. D., Monks, A., Tierney, S., Nofziger, T. H., Currens, M. J., Seniff, D., and Boyd, M. R. (1988) Evaluation of a soluble tetrazolium/formazan assay for cell growth and drug sensitivity in culture using human and other tumor cell lines. *Cancer Res.* **48,** 4827–4833

27. D'Alessio, D. A., Verchere, C. B., Kahn, S. E., Hoagland, V., Baskin, D. G., Palmiter, R. D., and Ensinck, J. W. (1994) Pancreatic expression and secretion of human islet amyloid polypeptide in a transgenic mouse. *Diabetes* **43,** 1457–1461
28. Bendrik, C., Robertson, J., Gauldie, J., and Dabrosin, C. (2008) Gene transfer of matrix metalloproteinase-9 induces tumor regression of breast cancer in vivo. *Cancer Res.* **68,** 3405–3412
29. Meier, D. T., Entrup, L., Templin, A. T., Hogan, M. F., Samarasekera, T., Zraika, S., Boyko, E. J., and Kahn, S. E. (2015) Determination of optimal sample size for quantification of beta-cell area, amyloid area and beta-cell apoptosis in isolated islets. *J. Histochem. Cytochem.* **63,** 663–673
30. Wiltzius, J. J., Sievers, S. A., Sawaya, M. R., Cascio, D., Popov, D., Riekel, C., and Eisenberg, D. (2008) Atomic structure of the cross-beta spine of islet amyloid polypeptide (amylin). *Protein Sci.* **17,** 1467–1474
31. Abedini, A., Meng, F., and Raleigh, D. P. (2007) A single-point mutation converts the highly amyloidogenic human islet amyloid polypeptide into a potent fibrillization inhibitor. *J. Am. Chem. Soc.* **129,** 11300–11301
32. Scrocchi, L. A., Chen, Y., Waschuk, S., Wang, F., Cheung, S., Darabie, A. A., McLaurin, J., and Fraser, P. E. (2002) Design of peptide-based inhibitors of human islet amyloid polypeptide fibrillogenesis. *J. Mol. Biol.* **318,** 697–706
33. Cao, P., Meng, F., Abedini, A., and Raleigh, D. P. (2010) The ability of rodent islet amyloid polypeptide to inhibit amyloid formation by human islet amyloid polypeptide has important implications for the mechanism of amyloid formation and the design of inhibitors. *Biochemistry* **49,** 872–881
34. Potter, K. J., Scrocchi, L. A., Warnock, G. L., Ao, Z., Younker, M. A., Rosenberg, L., Lipsett, M., Verchere, C. B., and Fraser, P. E. (2009) Amyloid inhibitors enhance survival of cultured human islets. *Biochim. Biophys. Acta* **1790,** 566–574
35. MacArthur, D. L., de Koning, E. J., Verbeek, J. S., Morris, J. F., and Clark, A. (1999) Amyloid fibril formation is progressive and correlates with beta-cell secretion in transgenic mouse isolated islets. *Diabetologia* **42,** 1219–1227
36. Zraika, S., Hull, R. L., Udayasankar, J., Aston-Mourney, K., Subramanian, S. L., Kisilevsky, R., Szarek, W. A., and Kahn, S. E. (2009) Oxidative stress is induced by islet amyloid formation and time-dependently mediates amyloid-induced beta cell apoptosis. *Diabetologia* **52,** 626–635
37. Luca, S., Yau, W. M., Leapman, R., and Tycko, R. (2007) Peptide conformation and supramolecular organization in amylin fibrils: constraints from solid-state NMR. *Biochemistry* **46,** 13505–13522
38. Nilsson, M. R., and Raleigh, D. P. (1999) Analysis of amylin cleavage products provides new insights into the amyloidogenic region of human amylin. *J. Mol. Biol.* **294,** 1375–1385
39. Jaikaran, E. T., Higham, C. E., Serpell, L. C., Zurdo, J., Gross, M., Clark, A., and Fraser, P. E. (2001) Identification of a novel human islet amyloid polypeptide beta-sheet domain and factors influencing fibrillogenesis. *J. Mol. Biol.* **308,** 515–525
40. Maurer-Stroh, S., Debulpaep, M., Kuemmerer, N., Lopez de la Paz, M., Martins, I. C., Reumers, J., Morris, K. L., Copland, A., Serpell, L., Serrano, L., Schymkowitz, J. W., and Rousseau, F. (2010) Exploring the sequence determinants of amyloid structure using position-specific scoring matrices. *Nat. Methods* **7,** 237–242
41. Fernandez-Escamilla, A. M., Rousseau, F., Schymkowitz, J., and Serrano, L. (2004) Prediction of sequence-dependent and mutational effects on the aggregation of peptides and proteins. *Nat. Biotechnol.* **22,** 1302–1306
42. Glenner, G. G., Eanes, E. D., and Wiley, C. A. (1988) Amyloid fibrils formed from a segment of the pancreatic islet amyloid protein. *Biochem. Biophys. Res. Commun.* **155,** 608–614
43. Haataja, L., Gurlo, T., Huang, C. J., and Butler, P. C. (2008) Islet amyloid in type 2 diabetes, and the toxic oligomer hypothesis. *Endocr. Rev.* **29,** 303–316
44. Weise, K., Radovan, D., Gohlke, A., Opitz, N., and Winter, R. (2010) Interaction of hIAPP with model raft membranes and pancreatic beta-cells: cytotoxicity of hIAPP oligomers. *Chembiochem.* **11,** 1280–1290
45. Chen, M. S., Zhao, D. S., Yu, Y. P., Li, W. W., Chen, Y. X., Zhao, Y. F., and Li, Y. M. (2013) Characterizing the assembly behaviors of human amylin: a perspective derived from C-terminal variants. *Chem. Commun.* **49,** 1799–1801
46. Abedini, A., and Schmidt, A. M. (2013) Mechanisms of islet amyloidosis toxicity in type 2 diabetes. *FEBS Lett.* **587,** 1119–1127
47. Masters, S. L., Dunne, A., Subramanian, S. L., Hull, R. L., Tannahill, G. M., Sharp, F. A., Becker, C., Franchi, L., Yoshihara, E., Chen, Z., Mullooly, N., Mielke, L. A., Harris, J., Coll, R. C., Mills, K. H., Mok, K. H., Newsholme, P., Nuñez, G., Yodoi, J., Kahn, S. E., Lavelle, E. C., and O'Neill, L. A. (2010) Activation of the NLRP3 inflammasome by islet amyloid polypeptide provides a mechanism for enhanced IL-1beta in type 2 diabetes. *Nat. Immunol.* **11,** 897–904
48. Westermark, G. T., Davalli, A. M., Secchi, A., Folli, F., Kin, T., Toso, C., Shapiro, A. M., Korsgren, O., Tufveson, G., Andersson, A., and Westermark, P. (2012) Further evidence for amyloid deposition in clinical pancreatic islet grafts. *Transplantation* **93,** 219–223
49. Andersson, A., Bohman, S., Borg, L. A., Paulsson, J. F., Schultz, S. W., Westermark, G. T., and Westermark, P. (2008) Amyloid deposition in transplanted human pancreatic islets: a conceivable cause of their long-term failure. *Exp. Diabetes Res.* **2008,** 562985